






Shear Performance of GFRP Reinforced Concrete Beams with Seawater and Chopped Fiber

Waleed Abdallah¹, Abdelrahman M. Farrag^{1*}, Ahmed F. Deifalla² ,
Amal. H. Ibrahim¹, Hamdy M. Mohamed¹ , Ahmed H. Ali¹ 

¹ Department of Civil Engineering, Faculty of Engineering, Helwan University, Cairo 11382, Egypt.

² Structural Engineering and Construction Management Department, Future University in Egypt, Cairo 11835, Egypt.

Received 11 January 2023; Revised 06 March 2023; Accepted 19 March 2023; Published 01 April 2023

Abstract

This paper reports an experimental study on the behavior and shear strength of concrete beams reinforced with longitudinal GFRP bars mixed with sea water. In order to evaluate how much concrete contributes to shear resistance, seven beams were tested in bending. Similar in size and concrete strength, the beams were longitudinally reinforced with glass fiber-reinforced polymer bars; however, they did not even have shear reinforcement. The beams, which measured 3,100 mm in length, 400 mm in depth, and 200 mm in width, were conducted and tested up to failure. The test variables were longitudinal reinforcement ratios (1.0, 1.4, and 2.0%), chopped fiber content (0, 0.5, 2, and 3 kg/m³), and mixing water type (freshwater and seawater). The test findings showed that increasing the reinforcement ratio increased the neutral-axis depth and allowed the formation of more closely spaced fractures while decreasing the loss of flexural stiffness after cracking. By increasing the area of concrete in compression, this in turn enhances the contribution of aggregate interlock as well as the contribution of uncracked concrete. Furthermore, increasing the reinforcement ratio improves the dowel action, which reduces the tensile stresses that are created in the concrete around it.

Keywords: Seawater; Chopped Fiber; Fiber-Reinforced Polymer (FRP); Shear Strength.

1. Introduction

Increasingly global concerns about the accumulation of construction and demolition waste and the deterioration of reinforced concrete (RC) structures due to steel corrosion impose the need to use alternative "greener" materials to achieve more efficient and sustainable RC structures. Beams are usually reinforced with shear reinforcement to prevent shear failures. Due to the labor cost associated with reinforcement installation, shear reinforcement is usually expensive. Noncorrosive fiber-reinforced polymer (FRP) reinforcing bars are becoming more frequently used in place of steel reinforcing bars in a variety of applications, including marine construction, parking buildings, and bridges [1]. Additionally, in the field of tunnel excavation, the usage of glass-FRP (GFRP) bars and spirals in soft-eyes is growing in popularity in North America. Numerous studies looking into the contribution of concrete to the overall shear capacity of FRP concrete structures have been conducted recently. The experimental work has focused mainly on beams with rectangular cross sections mixed with fresh water [1–4]. Accordingly, many models have been put forward to calculate shear capacity, most often based on a statistical curve fit to experimental beam test results [5]. In addition, several guidelines and standards have been published, including empirical formulae for assessing the concrete shear contribution [6–9].

* Corresponding author: abdelrahman.magdy@buc.edu.eg

 <http://dx.doi.org/10.28991/CEJ-2023-09-04-05>



© 2023 by the authors. Licensee C.E.J, Tehran, Iran. This article is an open access article distributed under the terms and conditions of the Creative Commons Attribution (CC-BY) license (<http://creativecommons.org/licenses/by/4.0/>).

The aggregate interlock, uncracked concrete, residual tensile stress, and dowel-action mechanisms all contribute to the section's shear resistance in general, which is represented by the concrete shear contribution. The degree to which these mechanisms contribute is determined by the crack width, which is a result of the tension reinforcement's strain and the crack spacing [10, 11]. Some of the shear force in the member is absorbed by the longitudinal reinforcing bars. The reinforcing bars will behave like dowels as a result of this transverse loading, which also subjects them to bending and shearing. The vertical displacements of the bottom reinforcement bars along the diagonal fracture surface that result in members with transverse reinforcement are constrained, and dowel action significantly increases shear resistance. Dowel action is typically less significant when there is no shear reinforcement because the greatest shear in a dowel is constrained by the tensile strength of the concrete cover holding the dowel. When using a lot of longitudinal reinforcement, especially when it's placed over several layers [12], dowel action may be a significant factor. The quantity of dowel forces that can be employed in a certain circumstance is quite difficult to calculate. Several experimental studies on the operation of dowels revealed that the dowel shear force ranges from 15% to 25% of the total shear force [12]. Without web reinforcing, the longitudinal reinforcement ratio determines the shear strength of concrete elements.

This is explained by the fact that members with low reinforcement ratios experience broader and deeper cracks than those with high reinforcement ratios. By lowering the residual tensile stress and aggregation interlock in the fractured surface, wider cracks lessen the interface shear. Deeper fractures, on the other hand, diminish the depth of the compression zone of uncracked concrete, which lowers the contribution of uncracked concrete to the shear strength. Additionally, due to the wider use of seawater in structural concrete, it is hypothesized to have direct environmental advantages. Arosio et al. [13] reported that concrete's water footprint could be reduced by up to 12% by mixing it with seawater. According to studies, the longer service life of FRP in concrete structures also clearly benefits the environment [14–16]. For instance, Cadenazzi et al. [15] reported that using GFRP rather than black steel to reinforce concrete bridges results in decreases in cradle-to-grave global warming (by 25%), photochemical oxidant production (by 15%), acidification (by 5%), and eutrophication (by 50%). Together, these materials might provide significant economic advantages in addition to environmental advantages. According to a life-cycle cost estimate of seawater-mixed GFRP-reinforced concrete for high-rise buildings with a 100-year service life, the proposed concrete would be around 50% less expensive in the long run than conventional (i.e., concrete with freshwater and steel) [17].

Studies on seawater concrete have often shown a little reduction in the strength of the concrete over time (up to 10%), which is probably caused by the presence of specific ions in seawater (although these reductions depend on the curing regime used) [18–20]. However, these losses can be lessened by altering the mixture design, which includes using particular chemical admixtures in concrete [21, 22]. The long-term strength performance of GFRP bars in seawater concrete has also been confirmed by durability studies [23–25]. There are few studies on the shear behavior of RC beams with seawater and chopped fiber-mixed concrete.

Given its high strength-to-weight ratio, great durability performance, and significantly lower cost compared to carbon FRPs, GFRP has demonstrated high potential as a substitute for non-corrosive reinforcement [26]. Design standards have also been created for the use of GFRP bars in RC elements, and they have been successfully implemented in a variety of structures, including bridges, parking garages, tunnels, and marine assemblies [7, 27, 28]. crack formation, the contribution from dowel action declines as the reinforcement ratio is reduced.

Research on the shear behavior of concrete members reinforced with FRP bars is required in light of the discussion above. The experimental investigation described here is a component of a larger, on-going program of research at Helwan University that tests seven RC beam reinforcement materials that were fabricated and tested under four-point loading to evaluate various variables and design variables.

2. Experimental Program

The present study is undertaken to experimentally investigate the contribution of concrete to the shear resistance of slender beams ($a/d > 2.5$) longitudinally reinforced by glass fiber reinforced polymer (GFRP) bars but without shear reinforcement. The reinforcement ratio, the amount of chopped fiber, and the type of mixing water were the test variables. The actual reinforcement ratio for the FRP-reinforced concrete beams is greater than the balanced reinforcement ratio, which is described in Section 8.2.1 of ACI 440.1R-03 as:

$$\rho_{fb} = 0.85\beta_1 \frac{f'_c}{f_{fu}} \frac{E_f \epsilon_{cu}}{E_f \epsilon_{cu} + f_{fu}} \quad (1)$$



Figure 1. Flowchart of the methodology

2.1. Test Specimens

The goal of the experimental work for this study was to get data on the shear behavior and strength of concrete beams reinforced with FRP bars that had been mixed with seawater but without web reinforcement. A total of seven RC beams, including five reinforced with 5 glass-FRP bars ($\rho = 1.0\%$), one with 7 glass-FRP bars ($\rho = 1.4\%$), and one with 10 glass-FRP bars ($\rho = 2.0\%$), were tested under two-point loading to determine the concrete contribution to their shear resistance. Figure 2 shows the dimensions, various configurations, and reinforcement details of the test specimens.

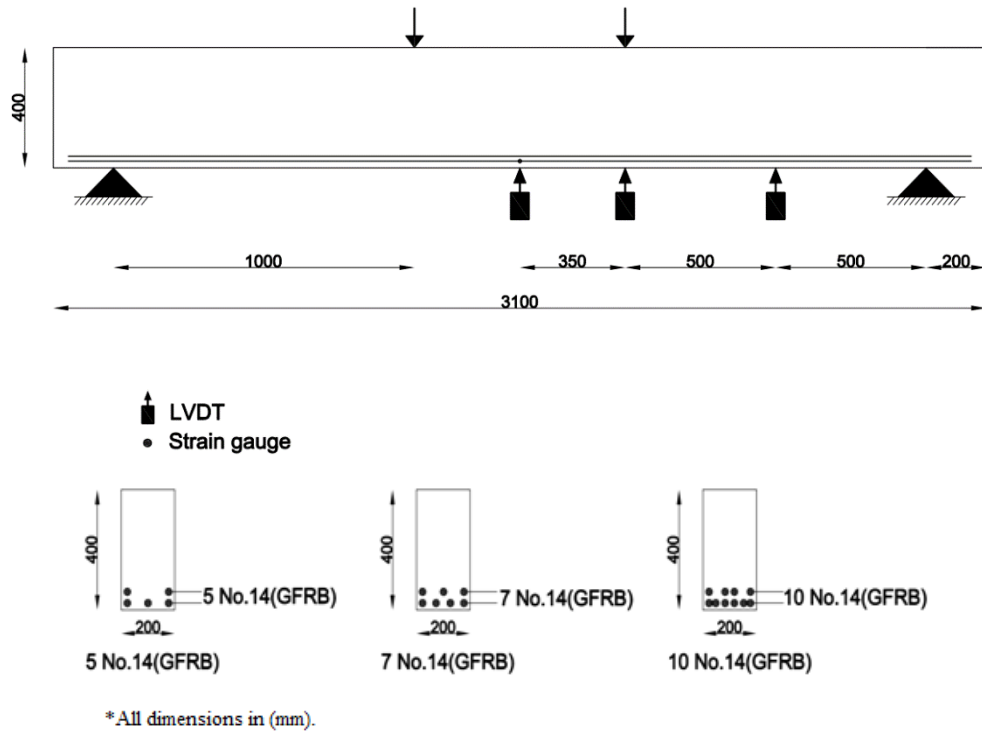


Figure 2. Test setup and cross-sectional details

Each beam was simply supported over a 2,700 mm span and had a total length of 3,100 mm, an equivalent effective flexural depth (d) of 375 mm, an equivalent effective shear depth ($d_v = 0.9d$) of 338 mm, depth of 400 mm, and width of 200 mm. The equivalent effective depths were estimated based on the shear provisions (Clause 5.8.2.9) in the 2012 edition of the *AASHTO LRFD Bridge Design Specifications*. The test parameters in this study included the effects of the reinforcement ratio, chopped fiber content, and mixing water type. The test matrix and reinforcing details for the beam specimens are shown in Table 1. The beams were designed to have a shear failure prior to flexure failure. The GFRP bars of diameter #14.0 mm were used as longitudinal reinforcement for all the tested beams.

Table 1. Details of the tested beams

Beam	Bottom Reinforcement (%)		Mixing water (Freshwater/Seawater)	Chopped Fiber Content (kg/m ³)
	Straight	ρ_f %		
AI	5Ø14	1	Freshwater	0
BI	7Ø14	1.4	Freshwater	0
CI	10Ø14	2	Freshwater	0
AII	5Ø14	1	Freshwater	0.5
AIII	5Ø14	1	Freshwater	2
AIV	5Ø14	1	Freshwater	3
AV	5Ø14	1	Seawater	0

2.2. Material Properties

The E-glass fibers utilized in the pultrusion procedure to produce the GFRP bars used in this research were impregnated with a modified vinyl-ester resin. High-modulus (HM) GFRP bars (CSA S807-10 Grade III) of 14 mm designated diameter were used in this study, as shown in Figure 3. The fiber contents in percentage by weight were 80

for the GFRP. The tensile strength and elastic modulus were calculated using the nominal cross-sectional area. The concrete used to cast each beam specimen was normal-weight concrete. The following mixture proportions were used per cubic meter of concrete: 1051 kg of coarse aggregate with a size range of 10 to 20 mm, 672 kilograms of fine aggregate, 430 kg of cement, a water-cement ratio (w/c) of 0.39, 301 mL of air entrainer, and 860 mL of water-reducing agent. Before casting, the slump was 80 mm. After 28 days, the concrete had reached the desired 35 MPa compressive strength. The actual compressive strength was calculated using the average test results of five concrete cylinders (each measuring 100 × 200 mm) tested on the same day as the start of the beam specimen testing.



Figure 3. GFRP bars

2.3. Details of Beam Fabrication

For the tested beams, seven GFRP cages were assembled. The 40 mm clear concrete cover remained unchanged. In wood formwork, the beams were prepared for casting. As shown in Figure 4, the formwork was positioned horizontally, and concrete was cast from the top. Vibration from both inside and outside was utilized. The fabrication procedure before and after casting is shown in Figure 4.



Figure 4. Fabrication process before and after casting

2.4. Instrumentation and Test Setup

With gauge lengths of 10 mm, electrical-resistance strain gauges were used to measure the strains in the longitudinal bars. Additionally, strain gauges were positioned on every shear span to gauge the diagonal strains in the concrete at the mid-shear span. Beam deflection was measured with three LVDTs placed at the mid-span and mid-shear span. The crack width was monitored by visual inspection during the test until the first crack appeared, which was initially measured with a handheld microscope. Then, seven high-accuracy LVDTs (± 0.001 mm) were installed at the crack location (three at each shear span and one at the mid-span). The test setup was designed and fabricated in Helwan University's structural laboratory. A servo-controlled, hydraulic 500 kN MTS actuator connected to a spreader beam was used to load the beams in four-point bending, as shown in Figure 5. A displacement-controlled rate of 1.0 mm/min was used to apply the load. The readings of the LVDTs, load cells, and strain gauges were captured by an automatic data acquisition system controlled by a computer.



Figure 5. Experimental test setup

3. Observations, Results, and Discussion

In the discussion, the measured concrete contribution to shear strength is represented by the notation (V_{exp}), and is equal to the maximum load P from the experiments. The load at which there is either a complete and abrupt failure or a sudden reduction in load carrying capability is referred to as the shear strength definition. Before the beam completely fails, a diagonal crack forms in one of the shear spans, which causes a sudden drop in load carrying capacity. Table 2 includes the test beams shear strength, (V_{exp}), as well as other relevant data. The experimental test findings in terms of deflection values and ultimate shear load (V_{exp}), and the measured strain in the longitudinal reinforcement (ϵ_u), modes of failure, and deflection, will be detailed in the following discussion includes the effect of the test variables on the ultimate shear strength and behavior of the tested beams.

Table 2. Experimental shear strength and deflection values for tested beams

Beam	Reinforcement		Mixing water (Freshwater/Seawater)	V_{EXP} . (ton)	Deflection (mm)		
	(ρ_f) %	No. of bars			At mid-span	Under point load	Between Point load and support
A-I	1	5	Freshwater	10.0659	17.653	15.745	8.304
B-I	1.4	7	Freshwater	11.148	12.423	11.643	6.784
C-I	2	10	Freshwater	13.87	7.534	6.347	5.326
AII	1	5	Freshwater	10.176	17.425	15.554	8.154
AIII	1	5	Freshwater	11.2	16.257	15.382	7.897
AIV	1	5	Freshwater	10.3	15.78	14.975	7.468
AV	1	5	Seawater	10.1994	16.754	15.724	8.075

3.1. Effect of Test Parameters on Load–Deflection Behavior

To illustrate the effects of various parameters on the shear behavior of RC-GFRP beams, as shown in Figure 6, this section presents the load-deflection curves for the tested beams in three groups. Before cracking, the tested beams exhibited linear load-deflection behavior. Using the gross moment of inertia of the concrete cross section, the stiffness of the beam at this stage was essentially comparable independent of the amount and type of reinforcement. As the load increased after cracking, stiffness decreased. At this stage, the longitudinal reinforcement's area and elastic modulus, which determine the axial stiffness of the reinforcing bars, were a factor in flexural stiffness, which was a function of those parameters [1].

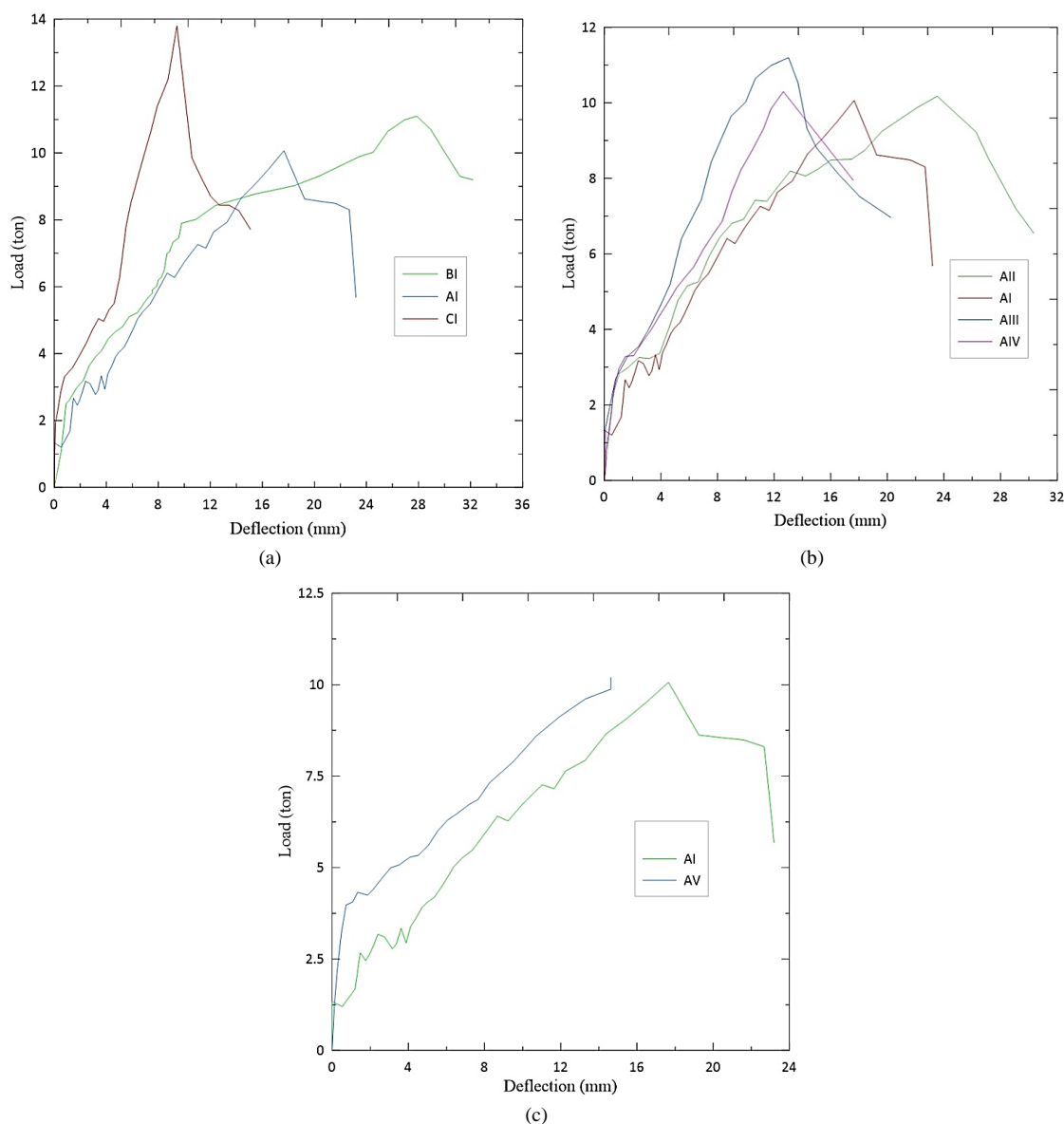
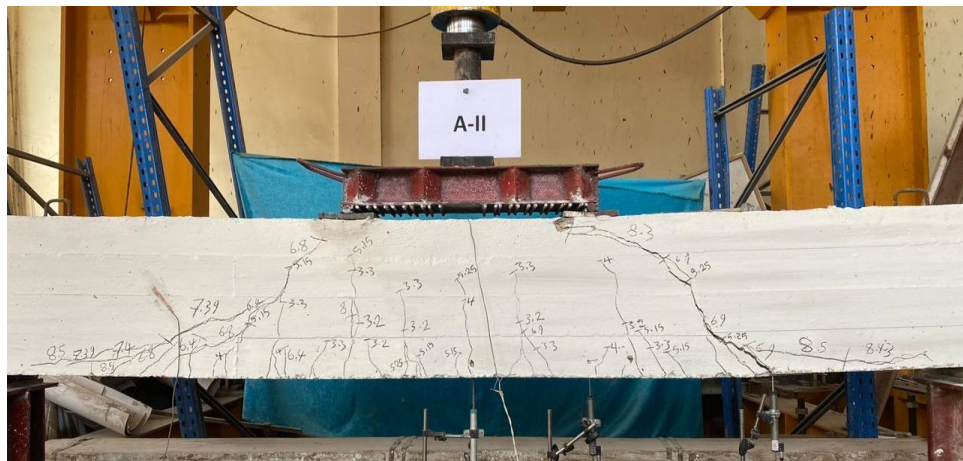


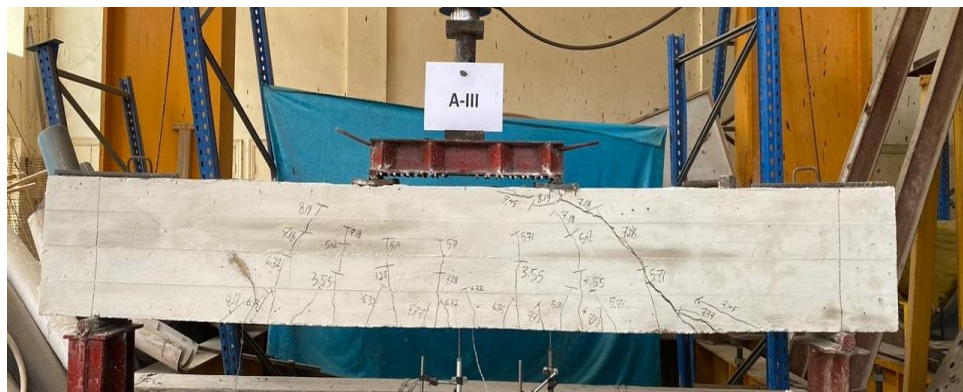
Figure 6. Effect of test parameters on load-deflection behavior

Figure 6-a shows the effect of reinforcement type on the load-deflection behavior. The three GFRP reinforced beams (A-I, B-I, and C-I) were designed to have a flexural-reinforcement ratio as 1%, 1.4%, and 2.0%, respectively. Nevertheless, the increase in deflection immediately after cracking was more significant in the GFRP-reinforced beams with a lower reinforcement ratio of 1%. This illustrates the effect of the reinforcing bars' elasticity modulus on the stiffness of the flexural after-cracking. The figure demonstrates that the post-cracking flexural stiffness for the beam strengthened with 5 GFRP bars (1%) was lower than that of the beam reinforced with 10 GFRP bars (2.0%). The average ratio between the post-cracking flexural stiffness of the GFRP-reinforced beam with a 2.0% reinforcement ratio to the GFRP-reinforced beam with 1% reinforcement ratio was approximately 1.45. These ratios were approximately the same as the ratios of the modulus of elasticity of steel to that of FRP bars. Therefore, it can be concluded that the post-cracking flexural stiffness was equal to the ratio of the axial stiffness of the FRP reinforcing bars. This is in good agreement with the results of Ali et al. [1], Tureyen & Frosch [2] and El-Sayed Ahmed [3]. Figure 6-a, indicate that, after cracking, the flexural stiffness of the GFRP-RC beams CI ($k_u = 31.5$ kN/m) and BI ($k_u = 23.6$ kN/m) was almost 3 and 2.3 times of that of the GFRP-RC beam AI ($k_u = 10.2$ kN/m). Thus, the flexural behavior of the tested beams seems to have been a function of the axial stiffness of the reinforcing bars. Since the deflection behavior of a beam reflects its stiffness inversely proportions to it, according to the slope of the initial deflection at the linear stage of loading, the beam (C1) had an initial stiffness more than the (AI and BI) by 45%.

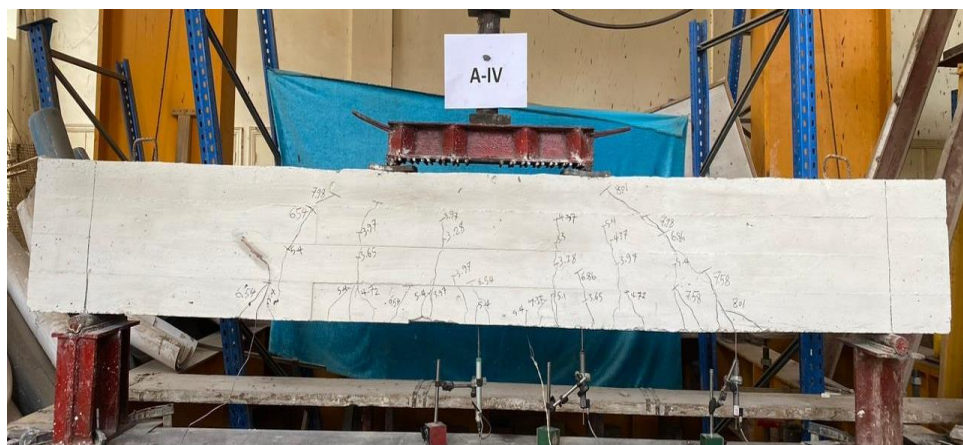
The effect of chopped fibers on the behavior and strength of FRP-reinforced concrete beams is shown in Figure 6-b. As shown in Figure 6-b, which illustrates that when adding chopped fibers by 2 and 3 kg/m³, the ultimate load and stiffness of the beam increased while the deflection decreased at the same load level. These results show the good response of specimens having chopped fibers, especially the 3 kg/m³ ones, compared with those that have not. The



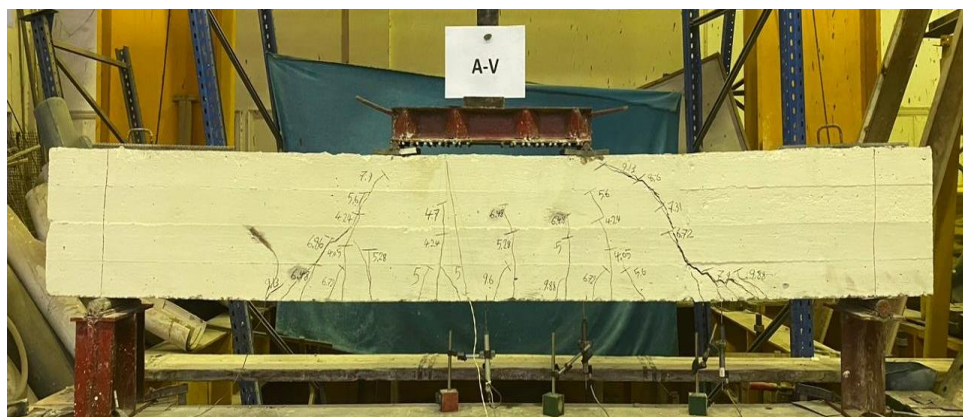
(d)



(e)



(f)

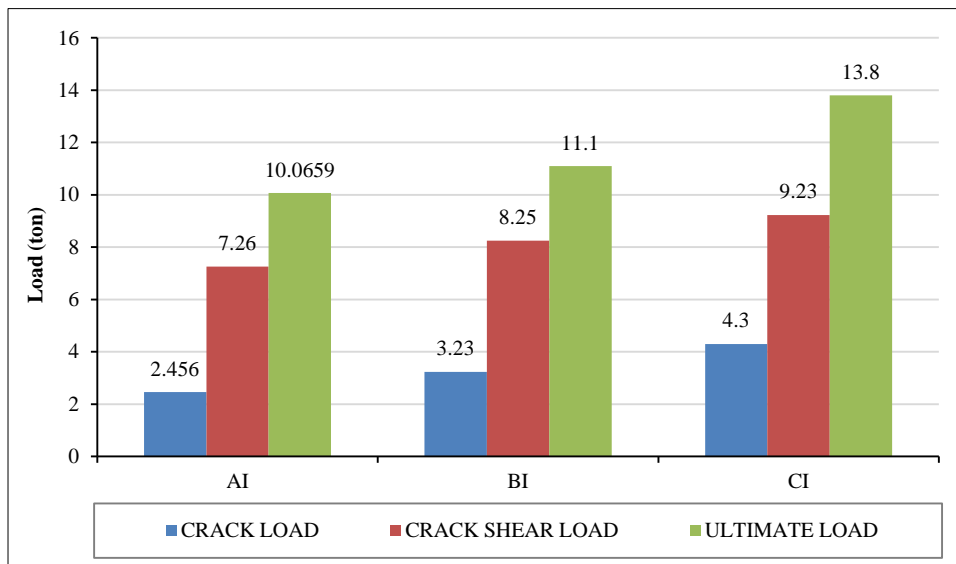


(g)

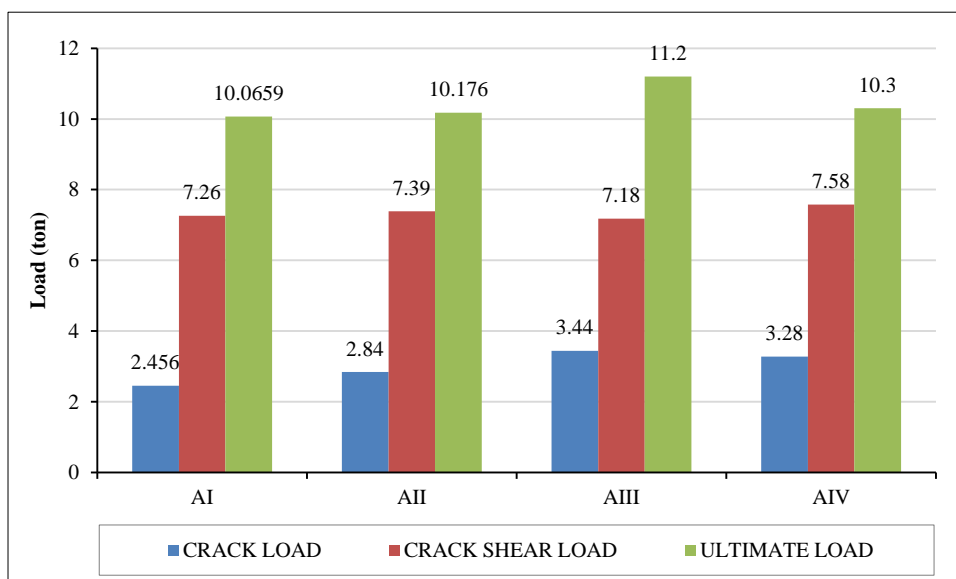
Figure 7. Crack pattern and modes of failure

It's observed that the failure modes for the beams were almost similar, it happened at the shear zone. Upon increasing the load, more flexure cracks appeared in the bottom of the tension zone and expanded vertically upward. After that at different loading stages, the flexural-shear cracks propagated and increased in number at a higher rate than their vertical expanding. Then the shear cracks began to propagate at a higher rate. Also shear cracks occurred at the top of the beam below the loading points at high loading stages. The shear cracks expanded gradually until they caused the shear failure for the concrete.

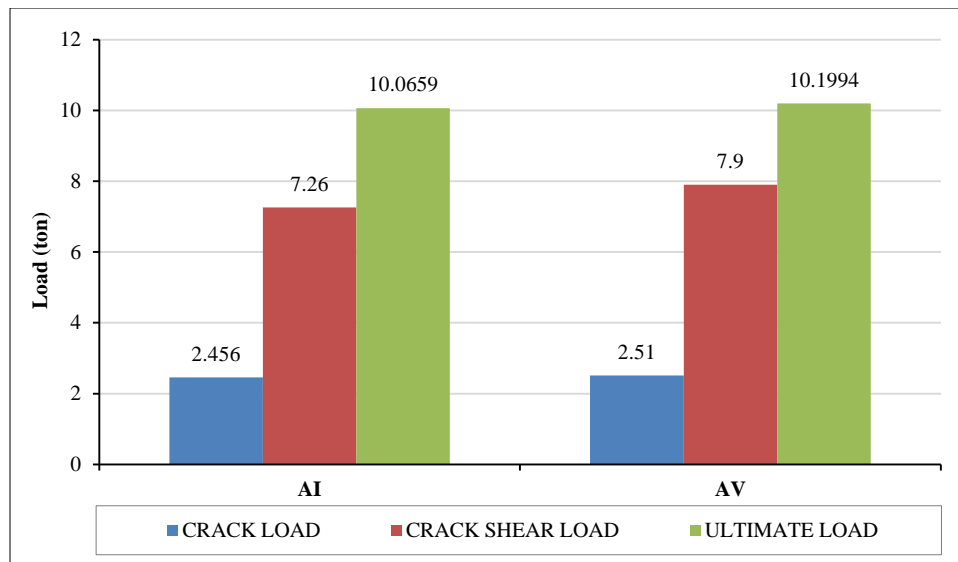
The first crack in beams (AI, BI, CI) was discovered at mid-span bottom fiber by 2.4-, 3.2- and 4.3-ton load respectively as shown in Figure 8-a. Regardless of the type of reinforcement, it was generally found that specimens with lower reinforcement ratios (AI) failed in brittle shear with few visible diagonal shear cracks. The specimens (BI and CI) with larger reinforcement ratios showed less brittle shear failure and the formation of many diagonal cracks. The final cracking pattern for each test specimen is shown in Figure 7. The thick lines show cracks that developed at failure, while the lighter ones show cracks that developed earlier. In a specimen with a high reinforcement ratio, severe cover spalling was seen at the ultimate load on the upper surface of the beam (CI). This is explained by the fact that, when shear failure was about to occur, more inclined upper cracks spread from the diagonal-tension shear crack back towards the support. The opening of the inclined failure crack effectively causes the aggregate interlock to be lost, hence the net shear transfer was dispersed across the section. To maintain cross-sectional equilibrium, the longitudinal reinforcement's dowel action, which was distributed evenly throughout the section, had to be increased. The concrete around the bars experienced a vertical tensile stress as a result of the sudden increase in dowel action in these bars. This was significant enough to cause cover spalling and splitting along the plane of the reinforcement when combined with the existing splitting stresses put on by the flexural bond.



(a)



(b)



(c)

Figure 8. Comparison of the cracking, shear crack and ultimate loads for beams

For beams (AI, AII, AIII and AIV and AV), the first crack was observed in the mid-span at 2.4, 2.8, 3.44 and 3.28 and 2.51 ton load respectively as observed in Figure 8-b. It's shown that, At the chopped fiber content of 0.5, 2 and 3 kg/m³, the cracking load was greater than the cracking load of the specimen AI with 0 kg/m³ by 4%, 10% and 8% respectively. However, when the chopped fiber content increases from 2 to 3 kg/m³ the cracking load decreases by 9%, and this would be explained by that the chopped fiber content with a high ratio may not be mixed well with the concrete specially with chopped glass fiber which may causes a void and be a weak zone in tension in the concrete. So, it must be sure that the chopped fiber is well distributed in the concrete to reach the required homogeneity.

At the mid-span for beams (AI and AV), the first crack was obtained at 2.4- and 2.51-ton load respectively as shown in Figure 8-c. We can find that using in concrete mixtures has little to no effect in the short-term on the cracking load instead of using freshwater. using seawater increases the cracking load than using freshwater by 2% and 3% respectively.

3.3. Shear Capacity of Concrete Beams

The definition of shear failure used herein describes the formation of inclined shear (diagonal-tension) cracking and the subsequent sudden drop in load-carrying capacity. Shear capacity is defined as the load at which complete or abrupt failure occurs [29]. Beams (AI, BI and CI) failed in diagonal tension. Figure 8-a, and Figure 9 give the effect of the reinforcement ratio on the shear strength of the tested beams.

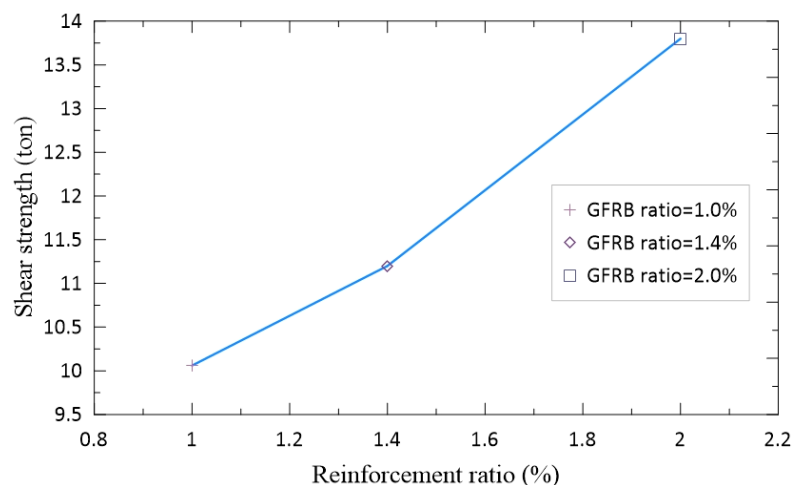


Figure 9. Shear strength versus reinforcement ratio

The figures show that as the reinforcement ratio increased, the shear strength of the GFRP-reinforced beams increased. Shear strengths increased by 11.0% and 37%, respectively, when the reinforcement ratio was increased by about 40% and 100% (from 1.0% to 1.4% and from 1.0% to 2.0%). The shear strengths were also increased by 24% by increasing the reinforcement ratio by 40% (from 1.4% to 2.0%). For the beam with the highest reinforcement ratio, the

increase in shear strength was more pronounced. By increasing the neutral-axis depth and enabling the formation of more closely spaced cracks, the use of additional reinforcement dispersed across the cross section reduces the loss of flexural stiffness after cracking. By increasing the area of concrete in compression, this in turn enhances the contribution of aggregate interlock as well as the contribution of uncracked concrete. Furthermore, raising the reinforcement ratio improves the dowel action, which reduces the tensile stresses which are created in the surrounding concrete.

Beams (AI, AII, AIII and AIV) failed in diagonal tension. Figure 8-b gives the effect of the chopped fiber on the shear strength of the tested beams. The figure indicates that the shear strength in the GFRP-reinforced beams increased as the chopped fiber increased till the content of 2 kg/m³, after that the shear strength decreases when the chopped fiber content increases to 3 kg/m³. Increasing the chopped fiber content (from 0 to 0.5 kg/m³, from 0 to 2.0 kg/m³ and from 0 to 3.0 kg/m³) increased the shear strengths by 1.0%, 11% and 2%, respectively. However, increasing the chopped fiber content (from 2 to 3 kg/m³) decreased the shear strengths by 8%.

Beams (AI and AV) failed in diagonal tension. Figure 8-c gives the effect of the mixing water type on the shear strength of the tested beams. The figure indicates that the shear strength in the GFRP-reinforced beams had a slightly increasing with seawater mixing. Seawater mixing increased the short term of shear strengths by 1.0%.

3.4. Strains in the FRP Longitudinal Reinforcement

For the internal GFRP longitudinal bars, Figure 10 shows the measured applied load on the beams versus the strain relationships.

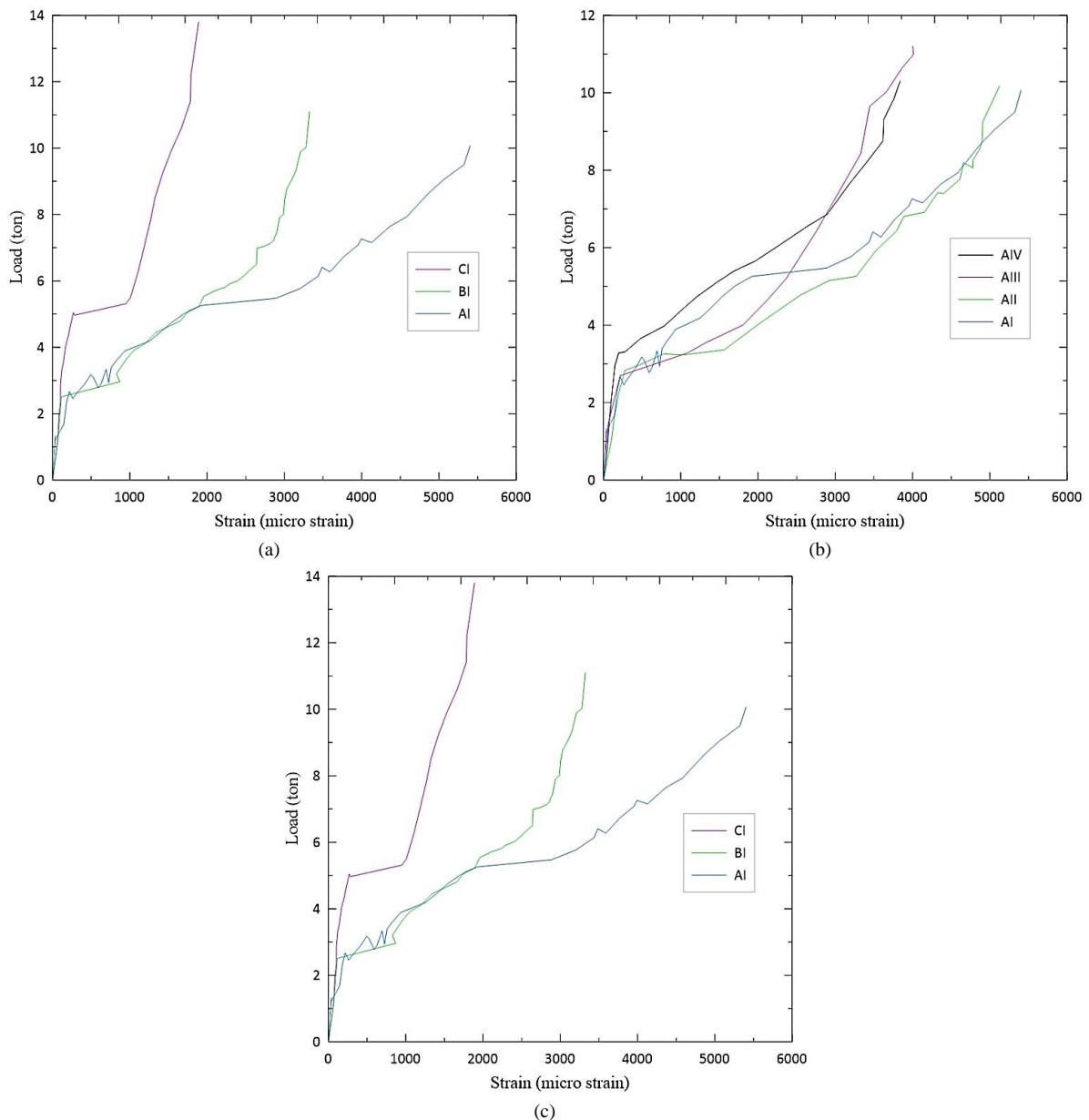


Figure 10. GFRP bar stress-strain relationship

For beams (AI, BI and CI) the longitudinal reinforcing bars of the FRP specimens had very little strain up until the concrete section cracked, as illustrated in Figure 10-a. Up until this phase, the GFRP specimens showed strain behaviors that were comparable. At the same load level, after cracking the concrete beam reinforced with a greater reinforcement ratio (CI) showed less bar strain than the beams reinforced with FRP (AI and BI), as the latter had relatively lower elastic moduli than the specimen CI. Throughout the testing, no specimen's FRP longitudinal reinforcement strain reached 50% of the ultimate tensile strain of the bars. None of the beams showed any indications of anchorage issues. The maximum strains in FRP bars were approximately 5450, 3300, and 1900, microstrains for AI, BI, and CI, respectively. In general, this relatively low strain at ultimate in the beams reinforced with FRP bars shows that shear failure was not triggered by the FRP bars rupturing.

For beams (AI, AII, AIII and AIV), up until the concrete section cracked, there was little strain in the longitudinal reinforcing bars of the FRP specimens. The concrete beams mixed with higher chopped fiber content (AIII and AIV) exhibited less bar strain than the beams mixed with lower chopped fiber content (AI and AII) at the same load level as shown in Figure 10-b. The maximum strains in FRP bars were approximately 5400, 5150, 4000 and 3850, microstrains for AI, AII, AIII and AIV, respectively.

For beams (AI and AV) up until the concrete section cracked, there was little strain in the longitudinal reinforcing bars of the FRP specimens as shown in Figure 10-c. The concrete beams mixed with seawater (AV) exhibited less bar strain than the beams mixed with freshwater (AI) at the same load level. The maximum strains in FRP bars were approximately 5450 and 4000, microstrains for AI, and AV, respectively.

3.5. Shear Crack Width

During the experimental test, it was found that increasing the reinforcement ratio minimized the shear-crack width. Therefore, at the same stress level, shear-crack width decreases as reinforcement ratio increases. Wider cracks were observed on the GFRP-reinforced beam (AI) the GFRP-reinforced one (BI and CI).

4. Conclusions

This paper presents experimental work to investigate the shear behaviour of beams reinforced with GFRP bars and mixed with seawater and chopped fiber. A total of seven full-scale RC specimens were prepared to study the effect of the reinforcement ratio, mixing water, and chopped fiber content on the shear behavior. Based on the experimental test results and analysis presented in this paper, the following conclusions can be drawn:

- Diagonal tension failure was the observed failure mode of the tested FRP reinforced beams.
- The axial stiffness of the reinforcing bars controls the load-deflection behavior of the beams after cracking.
- With an increase in the reinforcement ratio, the shear strength of beams increases.
- The axial stiffness of the longitudinal reinforcing bars affects how much concrete contributes to the shear strength of RC beams V_{cf} . The shear strength obtained increases with increasing reinforcement ratios or elastic modulus of the reinforcing bars.
- The cracking load of beams with 2% reinforcement ratio is 35% greater than 1% reinforcement ratio and beams with 1.4% reinforcement ratio is 15% greater than 1% reinforcement ratio.
- At the chopped fiber content of 0.5, 2 and 3 kg/m³, the cracking load was greater than the cracking load of the specimens with 0 kg/m³ by 4%, 10% and 8% respectively. However, when the chopped fiber content increases from 2 to 3 kg/m³ the cracking load decreases by 9%.
- The results suggest that the use of seawater in concrete has insignificant effects on the shear capacity of RC beams, using seawater increases the cracking load and cracking shear load than using freshwater by 2% and 3%, respectively. On the other hand, it increases the shear strength by 5%.

4.1. Recommendations

The results shown above, specifically the numbers, are based only on the materials and samples used in this investigation. Finally, it should be noted that the current study only evaluates the short-term shear performance of reinforced concrete beams. It is crucial that future research investigate the long-term effects of chemicals in seawater on GFRP-reinforced concrete beams. Further study is required to study the torsional and fatigue behaviors of reinforced concrete beams when reinforced with the proposed combination (seawater + chopped fiber + GFRP).

5. Declarations

5.1. Author Contributions

Conceptualization, W.A., A.H.A., H.M.M. and A.H.I.; methodology, W.A., A.M.F. A.H.A. and H.M.M.; writing—original draft preparation, A.M.F. and A.F.D.; writing—review and editing, A.M.F. and A.H.A.; supervision, W.A., A.H.A. and H.M.M. All authors have read and agreed to the published version of the manuscript.

5.2. Data Availability Statement

The data presented in this study are available in the article.

5.3. Funding

The authors received no financial support for the research, authorship, and/or publication of this article.

5.4. Acknowledgements

The authors would like to express their special thanks and gratitude for contribution of the technical staff of the structural lab in the Department of Civil Engineering at the Helwan University.

5.5. Conflicts of Interest

The authors declare no conflict of interest.

6. References

- [1] Ali, A. H., Mohamed, H. M., & Benmokrane, B. (2016). Shear Behavior of Circular Concrete Members Reinforced with GFRP Bars and Spirals at Shear Span-to-Depth Ratios between 1.5 and 3.0. *Journal of Composites for Construction*, 20(6), 04016055. doi:10.1061/(asce)cc.1943-5614.0000707.
- [2] Tureyen, A. K., & Frosch, R. J. (2002). Shear tests of FRP-reinforced concrete beams without stirrups. *Structural Journal*, 99(4), 427-434. doi:10.14359/12111.
- [3] El-Sayed Ahmed, A. K. (2007). Concrete contribution to the shear resistance of FRP-reinforced concrete beams. PhD Thesis, Université de Sherbrook, Sherbrook, Canada.
- [4] Razaqpur, A. G., & Isgor, O. B. (2006). Proposed shear design method for FRP-reinforced concrete members without stirrups. *ACI Structural Journal*, 103(1), 93. doi:10.14359/15090.
- [5] Hoult, N. A., Sherwood, E. G., Bentz, E. C., & Collins, M. P. (2008). Does the Use of FRP Reinforcement Change the One-Way Shear Behavior of Reinforced Concrete Slabs? *Journal of Composites for Construction*, 12(2), 125–133. doi:10.1061/(asce)1090-0268(2008)12:2(125).
- [6] Nanni, A. (2005). Guide for the Design and Construction of Concrete Reinforced with FRP Bars (ACI 440.1R-03). Structures Congress 2005. doi:10.1061/40753(171)158.
- [7] CSA-S806. (2012). Design and Construction of Building Components with Fibre-Reinforced Polymers. Canadian Standards Association (CSA), Toronto, Canada.
- [8] CSA-S807. (2010). Specification for Fibre-Reinforced Polymers. Canadian Standards Association (CSA), Toronto, Canada.
- [9] JSCE. (1997). Recommendation for design and construction of concrete structures using continuous fiber reinforcing materials. Japan Society of Civil Engineers, Tokyo, Japan.
- [10] Gouda, A., Ali, A. H., Mohamed, H. M., & Benmokrane, B. (2022). Analysis of circular concrete members reinforced with composite glass-FRP spirals. *Composite Structures*, 297, 115921. doi:10.1016/j.compstruct.2022.115921.
- [11] MacGregor, J. K., & Wight, J. G. (2005). Reinforced Concrete: Mechanics and Design (4th Ed.). Prentice-Hall, Upper Saddle River, United States.
- [12] ASCE-ACI Committee 445 on Shear and Torsion. (1998). Recent approaches to shear design of structural concrete. *Journal of structural engineering*, 124(12), 1375-1417. doi:10.1061/(asce)0733-9445(1998)124:12(1375).
- [13] Arosio, V., Arrigoni, A., & Dotelli, G. (2019). Reducing water footprint of building sector: Concrete with seawater and marine aggregates. *IOP Conference Series: Earth and Environmental Science*, 323(1), 12127. doi:10.1088/1755-1315/323/1/012127.
- [14] Zhang, C., Lin, W. X., Abududdin, M., & Canning, L. (2011). Environmental Evaluation of FRP in UK Highway Bridge Deck Replacement Applications Based on a Comparative LCA Study. *Advanced Materials Research*, 374–377, 43–48. doi:10.4028/www.scientific.net/amr.374-377.43.

- [15] Cadenazzi, T., Dotelli, G., Rossini, M., Nolan, S., & Nanni, A. (2019). Life-cycle cost and life-cycle assessment analysis at the design stage of a fiber-reinforced polymer-reinforced concrete bridge in Florida. *Advances in Civil Engineering Materials*, 8(2), 20180113. doi:10.1520/ACEM20180113.
- [16] Chen, L., Qu, W., & Zhu, P. (2016). Life cycle analysis for concrete beams designed with cross-sections of equal durability. *Structural Concrete*, 17(2), 274–286. doi:10.1002/suco.201400117.
- [17] Younis, A., Ebead, U., & Judd, S. (2018). Life cycle cost analysis of structural concrete using seawater, recycled concrete aggregate, and GFRP reinforcement. *Construction and Building Materials*, 175, 152–160. doi:10.1016/j.conbuildmat.2018.04.183.
- [18] Nishida, T., Otsuki, N., Ohara, H., Garba-Say, Z. M., & Nagata, T. (2015). Some Considerations for Applicability of Seawater as Mixing Water in Concrete. *Journal of Materials in Civil Engineering*, 27(7). doi:10.1061/(asce)mt.1943-5533.0001006.
- [19] Xiao, J., Qiang, C., Nanni, A., & Zhang, K. (2017). Use of sea-sand and seawater in concrete construction: Current status and future opportunities. *Construction and Building Materials*, 155, 1101–1111. doi:10.1016/j.conbuildmat.2017.08.130.
- [20] Dhondy, T., Remennikov, A., & Shiekh, M. N. (2019). Benefits of using sea sand and seawater in concrete: a comprehensive review. *Australian Journal of Structural Engineering*, 20(4), 280–289. doi:10.1080/13287982.2019.1659213.
- [21] Li, L. G., Chen, X. Q., Chu, S. H., Ouyang, Y., & Kwan, A. K. H. (2019). Seawater cement paste: Effects of seawater and roles of water film thickness and superplasticizer dosage. *Construction and Building Materials*, 229, 116862. doi:10.1016/j.conbuildmat.2019.116862.
- [22] Younis, A., Ebead, U., Suraneni, P., & Nanni, A. (2018). Fresh and hardened properties of seawater-mixed concrete. *Construction and Building Materials*, 190, 276–286. doi:10.1016/j.conbuildmat.2018.09.126.
- [23] El-Hassan, H., El-Maaddawy, T., Al-Sallamin, A., & Al-Saidy, A. (2018). Durability of glass fiber-reinforced polymer bars conditioned in moist seawater-contaminated concrete under sustained load. *Construction and Building Materials*, 175, 1–13. doi:10.1016/j.conbuildmat.2018.04.107.
- [24] El-Hassan, H., El-Maaddawy, T., Al-Sallamin, A., & Al-Saidy, A. (2017). Performance evaluation and microstructural characterization of GFRP bars in seawater-contaminated concrete. *Construction and Building Materials*, 147, 66–78. doi:10.1016/j.conbuildmat.2017.04.135.
- [25] Khatibmasjedi, M. (2018). Sustainable concrete using seawater and glass fiber reinforced polymer bars. PhD Thesis, University of Miami, Coral Gables, United States.
- [26] D'Antino, T., & Pisani, M. A. (2019). Long-term behavior of GFRP reinforcing bars. *Composite Structures*, 227, 111283. doi:10.1016/j.compstruct.2019.111283.
- [27] ACI440.1R-15. (2015). Guide for the Design and Construction of Structural Concrete Reinforced with Fiber-Reinforced Polymer (FRP) Bars. American Concrete Institute (ACI), Michigan, United States.
- [28] Ramesh, B., Eswari, S., & Sundararajan, T. (2021). Experimental and numerical studies on the flexural behaviour of GFRP laminated hybrid-fibre-reinforced concrete (HFRC) beams. *Innovative Infrastructure Solutions*, 6, 1-13. doi:10.1007/s41062-020-00374-z.
- [29] Yost, J. R., Goodspeed, C. H., & Schmeckpeper, E. R. (2001). Flexural Performance of Concrete Beams Reinforced with FRP Grids. *Journal of Composites for Construction*, 5(1), 18–25. doi:10.1061/(asce)1090-0268(2001)5:1(18).